A sustainable cobalt separation with validation by techno-economic analysis and life-cycle assessment

Boyang Zhang, Alexander B. Weberg, Andrew J. Ahn, Marta Guron, Leighton O. Jones, Michael R. Gau, Patrick J. Carroll, George C. Schatz, and Eric J. Schelter*

Abstract

Sustainable and cost-effective improvements to cobalt/nickel separations chemistry contribute to the realization of economically competitive lithium-ion battery recycling as well as primary mining of cobalt and nickel. Such improvements can address supply chain challenges associated with cobalt, a critical element. Herein, we disclose a simple method for separating Co/Ni by second coordination sphere molecular recognition. Selective cobalt precipitation is achieved using carbonate ions in ammonia solution due to the outer-sphere, non-covalent (hydrogen bonding) interactions between $[Co(NH_3)_6]^{3+}$ and CO_3^{2-}. We demonstrate the application of this method to mixtures of Co/Ni chlorides comprising a 10-fold excess of Ni and provide comparisons to ore-processing systems. High purities (99.4(3)% Co; 98.2(4)% Ni) and recoveries (77(8)% Co; ~100% Ni) were observed for both Co- and Ni-enriched products using optimized conditions. This method is potentially economically competitive based on initial TechnoEconomic Analysis (TEA) and Life-Cycle Assessment (LCA) that also illustrate advantages in terms of sustainability.

Introduction

Lithium-ion batteries (LIBs) are ubiquitous energy storage devices. Due to their relatively large energy densities, LIBs used in electric vehicles (EVs) represent one of the fastest growing sectors among clean energy technologies,[1] and have contributed to a significant reduction of greenhouse gas emissions from the transportation sector.[2] Nonetheless, a major challenge to the scaled use of LIBs is their requirements for critical elements, including lithium and cobalt.[3-5] In 2021, 63% of global Co demand was attributed to the production of cathode materials in LIBs, and 74% of the global light duty EV battery market was dominated by Ni/Co-containing devices.[6] The reliance on Co is problematic considering a shortage, based on estimated mineral reserves, for the United States to meet the demands for growth,[7] a projected global Co-shortage in the medium term,[6] environmental degradation from large-scale mining operations,[8] and ethical concerns surrounding the sourcing of Co from central Africa, especially the DR Congo.[9]

LIB recycling is a growing area of research that is expected to contribute to the supply chain challenges associated with Co sourcing by enabling a closed supply chain. Despite the significant advantages provided by LIB recycling, uncertain profitability at scale and lack of regulations and government support, among other reasons, have hindered widespread adoption to date.[10] A major challenge for valorizing Co from LIB waste streams, namely shredded and

processed battery cells called the "black mass," is the associated chemical separation of the metal components of black mass, such as Co, Ni, and Mn. Of the mixed-metal black mass separations problem, a chief challenge is Co/Ni separation, due to the chemical similarities of the elements.[11] Cost-effective and sustainable improvements to Co/Ni separations are needed to realize economically competitive LIB recycling.

In primary production, Co is commonly produced as a byproduct from hydrometallurgical processing of Ni-containing ores, particularly from laterite deposits (containing Fe, Ni, and Co) and sulfide ores (containing Co, Ni, and Cu). Hydrometallurgical Co/Ni separations are generally accomplished by one of three methods: chemical precipitation, ion exchange, or solvent extraction (SX), with the latter being the most commonly used.[12,13] However, because Co/Ni exhibit similar aqueous chemistries, current SX methods typically show modest selectivity and often require repeated extraction steps to obtain suitable Co purities. Additionally, SX processes require large solvent inventories, which can be both expensive and environmentally hazardous.[13,14] As such, despite the ability for SX systems to generate pure samples of Co and Ni at scale, improvements in Co separations especially in terms of selectivity, sustainability, and cost, are expected to contribute to developing LIB recycling technologies.

Selective precipitation has been garnering attraction as an alternative approach, especially in the context of precious metal recovery[15-19] and, more recently, group separation of rare-earth elements.[20,21] As an alternative approach, the advantages of selective precipitation include inherent simplicity, ease of scalability, and reduced energy demand and hazardous waste generation.[22] Existing studies of selective precipitation take advantage of second coordination-sphere, non-covalent interactions between the metal complex ion and the co-precipitant, typically a macrocyclic receptor. Subsequently, selective metal precipitation can be achieved by self-assembly of supramolecular structures in green solvents under ambient conditions. Herein, we disclose a simple, selective, and sustainable method for separating Co/Ni, without the use of organic solvents or expensive reagents. The selective precipitation of Co from aqueous media is achieved using aqueous ammonia and carbonate ions due to the selective secondary coordination sphere recognition. We demonstrate the application of this approach using mixtures of Co/Ni chlorides, with a 10-fold excess of Ni, and provide comparisons to the currently adopted ore-processing systems wherever possible. The separations chemistry described here is not only chemically competitive with the current state-of-the-art Co/Ni separations technologies, but also potentially economically competitive based on an initial technoeconomic analysis (TEA) performed in the current work, and offers clear advantages in terms of sustainability. This Co/Ni separations chemistry is expected to contribute to the growing LIB recycling as well as Co/Ni ore processing technologies.

Results

System design

Co^{II} and Ni^{II} ions display similar chemistries in aqueous media, but the application of coordination chemistry has been shown to differentiate properties of their complexes. For example, coordinating nitrogen donor ligands to these metals is known to cathodically shift the oxidation potentials such that Co^{II} complexes can be oxidized by air to the trivalent state, while Ni^{II} remains in the divalent one. These conditions generate the Co/Ni "Werner complexes" ($[Co(NH_3)_6]^{3+}$ and $[Ni(NH_3)_6]^{2+}$) that display exploitable chemical differences for SX. In addition to these thermodynamic differences ammonia ligands in $[Ni(NH_3)_6]^{2+}$ are labile and the complex demonstrates complete ligand exchange in aqueous ammonia in minutes,[23,24] whereas $[Co(NH_3)_6]^{3+}$ is kinetically inert demonstrating exchange rates orders of magnitude slower than $[Ni(NH_3)_6]^{2+}$.[25] Upon contacting aqueous $[Co(NH_3)_6]^{3+}$/$[Ni(NH_3)_6]^{2+}$ mixtures with an lipophilic extractant in an SX system, the ammonia ligands are displaced from $[Ni(NH_3)_6]^{2+}$ and the Ni is extracted into an organic phase by the formation of new coordination complexes with the extractant, whereas $[Co(NH_3)_6]^{3+}$ remains in the aqueous phase. While elegant in design and successful in application, this SX system presents limitations due to the requirements of SX processes discussed above.

We hypothesized that, besides differences in ligand lability between $[Co(NH_3)_6]^{3+}$ and $[Ni(NH_3)_6]^{2+}$, these complexes should also interact differently through intermolecular, non-covalent interactions. Specifically, we expected that the stronger Co–N interactions in $[Co(NH_3)_6]^{3+}$ should result in more acidic N–H bonds in the ammonia ligands, which should subsequently interact more strongly with hydrogen bond acceptors than the ammonia ligands in $[Ni(NH_3)_6]^{2+}$. Using an anionic hydrogen bond acceptor, such as carbonate, might therefore be expected to create an H-bonding network with $[Co(NH_3)_6]^{3+}$ of increased lattice energy, thereby leading to a selective precipitation of Co^{III} from mixtures of $[Co(NH_3)_6]^{3+}$ and $[Ni(NH_3)_6]^{2+}$.

Selective precipitation of $Co(NH_3)_6^{3+}$ with carbonate

Upon treatment of a solution of the trivalent complex $[Co(NH_3)_6][Cl]_3$ (5 mM) in concentrated aqueous ammonia with sodium carbonate (Na_2CO_3, 2 equiv), a yellow-orange precipitate was observed to form, leaving behind a colorless mother liquor (**Fig. 1a**). UV-Vis spectra of the mother liquor before and after Na_2CO_3 addition indicated an approximately quantitative precipitation of $[Co(NH_3)_6]^{3+}$ from solution (**Fig. 1b**). Similar results were observed when using either guanidinium carbonate (Gdm_2CO_3) or sodium bicarbonate. The precipitate obtained from Na_2CO_3 treatment of the $[Co(NH_3)_6]^{3+}$ solutions was found to be insoluble in aqueous ammonia, but soluble in neutral water. Notably, when the divalent Ni complex: $[Ni(NH_3)_6][Cl]_2$, (5 mM) was treated with carbonate under identical conditions, no precipitation was observed. Additionally, UV-Vis spectral features associated with $[Ni(NH_3)_6][Cl]_2$ before and after carbonate addition did not change over the course of several days (**Fig. 1a, 1c**). Experiments using larger quantities of carbonate and more concentrated $[Ni(NH_3)_6][Cl]_2$ (50 mM) likewise did not result in the formation of insoluble materials. The selectivity of the carbonate-induced precipitation for $[Co(NH_3)_6][Cl]_3$ over $[Ni(NH_3)_6][Cl]_2$ was consistent with our hypothesis that stronger ammonia bonding to the trivalent metal would display stronger intermolecular H-bonding

interactions, and prompted us to develop a Co/Ni separation based on selective precipitation under industrially-relevant conditions.

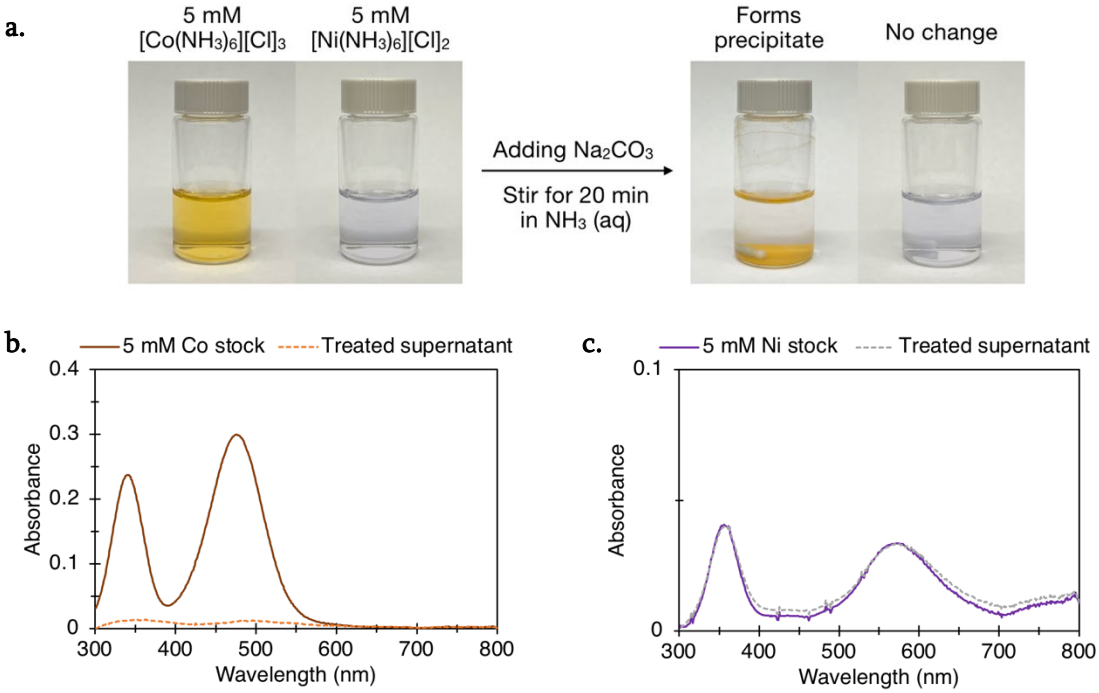

Fig. 1 Treatment of $[Co(NH_3)_6][Cl]_3$ or $[Ni(NH_3)_6][Cl]_2$ with Na_2CO_3. a Photos of the solutions of $[M(NH_3)_6]^{2+/3+}$ (M = Ni, Co) before and after carbonate addition. **b** UV-Vis spectra of the $[Co(NH_3)_6][Cl]_3$ solution (5 mM) before and after treatment with carbonate. **c** UV-Vis spectra of the $[Ni(NH_3)_6][Cl]_2$ solution (5 mM) before and after treatment with carbonate.

Structural characterization of the cobalt precipitate

Orange, X-ray quality single crystals of the Co precipitate were grown by combining Na_2CO_3 and $[Co(NH_3)_6][Cl]_3$ in aqueous ammonia. Alternatively, crystals obtained using Gdm_2CO_3 or $NaHCO_3$ in place of Na_2CO_3 were visually identical and displayed identical cubic unit cells. Elucidation of the solid-state structure of this material revealed the formation of a solid with the formula $[Co(NH_3)_6][Cl][CO_3]$ wherein two of the chloride anions in $[Co(NH_3)_6][Cl]_3$ were replaced by a single carbonate dianion (**Fig. 2a**). It should be noted that this structure was recently reported by Forbes and coworkers in a different context.[26] Hydrogen bonding between the ammonia ligands and the carbonate anions are prevalent throughout the structure (**Fig. 2b**), with each $[Co(NH_3)_6]^{3+}$ unit displaying six close contacts with neighboring carbonate anions (average $N_{ammonia}$–$O_{carbonate}$ distance = 2.87(2) Å) and three slightly longer contacts with neighboring carbonates ($N_{ammonia}$–$O_{carbonate}$ distance = 3.007(3) Å). Longer interactions between the chloride ion and $[Co(NH_3)_6]^{3+}$ were observed in the solid-state structure of $[Co(NH_3)_6][Cl][CO_3]$, with an average $N_{ammonia}$–Cl distance of 3.42(2) Å, suggesting weak H-bonding interactions. The H-

bonding throughout the structure likely contributes the precipitation of this material and suggests that analogous H-bonding / anion-cation interactions with the $[Ni(NH_3)_6]^{2+}$ cation are weaker. We therefore hypothesize that the selectivity of the precipitation event for Co over Ni is due to a combination of 1) the higher cationic charge density of the $[Co(NH_3)_6]^{3+}$ cation (3+ *versus* 2+), and 2) more acidic N–H bonds in the ammonia ligands due to stronger Co–NH_3 bonding.

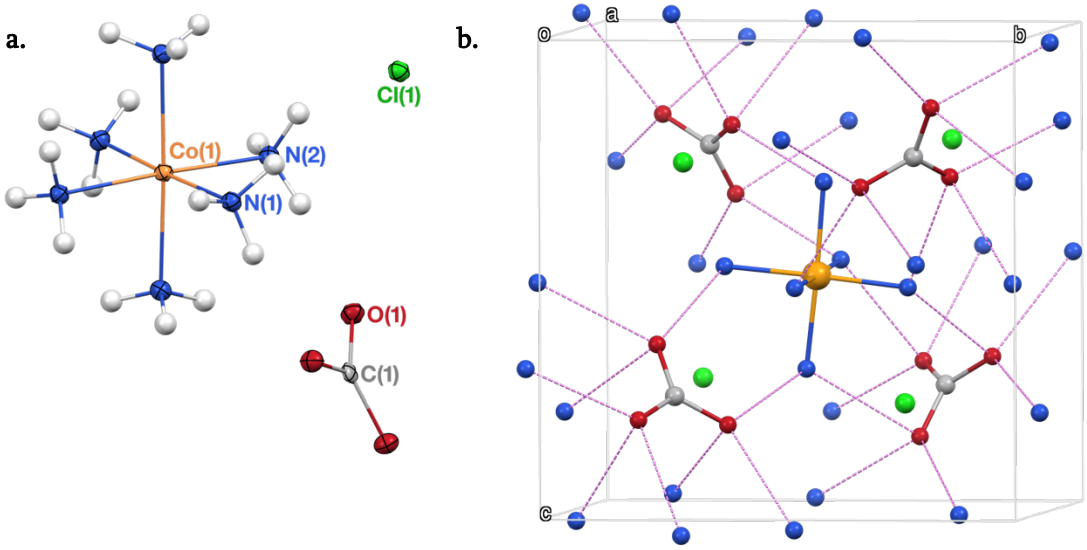

Fig. 2 Solid-state structure of $[Co(NH_3)_6][Cl][CO_3]$. Atom colors: orange = Co, blue = N, red = O, grey = C, green = Cl, white = H. **a** Solid-state structure of $[Co(NH_3)_6][Cl][CO_3]$, thermal ellipsoids depicted at 30% probability. **b** Depiction of the full unit cell of the $[Co(NH_3)_6][Cl][CO_3]$ solid-state structure. H-bonding interactions are highlighted with magenta dashed lines. Hydrogen atoms were omitted for clarity.

Computational analysis

Determining solubility properties from electronic structure (DFT) calculations is a complex and difficult undertaking where errors of less than 0.01 eV can be important in the balance between electrostatic, covalent and solvation interactions that lead to precipitation. However, a qualitative correlation was previously found between thermodynamic stability of complex+counterions and the ability of this material to precipitate,[22,27] so we use this approach in the present application. We use relatively high-level DFT and wavefunction-based methods to determine binding energies (**Supplementary Table 9 and 10**) and Energy Decomposition Analysis (EDA) (**Supplementary Table 8**) of the complexes and their anions. The results show consistent binding energy differences for the two levels of theory, with $[Co(NH_3)_6][Cl][CO_3]$ favored by about 4 eV per formula unit over $[Co(NH_3)_6][Cl]_3$ and by 15 eV over $[Ni(NH_3)_6][Cl]_2$. In addition, another property called bond order can inform us how strong a bond is. The metal-nitrogen bond orders were computed with three different approaches, namely Mayer, Gopinathan-Jug (G-J) and the first variant of Nalewajski-Mrozek (N-M1) approaches. The results show that $[Ni(NH_3)_6][Cl]_2$ has relatively lower orders overall (**Supplementary Tables 5–7**) as expected. Together, these results suggest that

the $[Co(NH_3)_6][Cl][CO_3]$ complex is the most stable structure and therefore the most likely to precipitate, which is what is experimentally observed.

Demonstration of a separation using Co/Ni$(NH_3)_6^{n+}$ n = 2 or 3

The separation of $[Co(NH_3)_6][Cl]_3$ from $[Ni(NH_3)_6][Cl]_2$ by carbonate-induced precipitation was demonstrated through treatment of a mixture of the complexes with either sodium carbonate or guanidinium carbonate. A 1:10 molar ratio of Co:Ni was chosen to mimic the nickel-rich environments commonly found in nickel laterite ores and in nickel manganese cobalt (NMC) LIB cathodes. A dark magenta solution containing 5 mM $[Co(NH_3)_6][Cl]_3$ and 50 mM $[Ni(NH_3)_6][Cl]_2$ in NH_4OH was prepared and treated with 3 equiv of either Na_2CO_3 or Gdm_2CO_3. A yellow-orange solid was observed to quickly precipitate upon stirring, leaving behind a bright violet solution (**Fig. 3a, 3b**). UV-Vis spectra of the mother liquor before and after carbonate addition indicated the bleaching of the spectral feature associated with $[Co(NH_3)_6][Cl]_3$ (λ = 476 nm), while spectral features associated with $[Ni(NH_3)_6][Cl]_2$ (λ = 571 nm) remained (**Fig. 3c** for Na_2CO_3, **Supplementary Fig. 1** for Gdm_2CO_3).

To gain more quantitative insight into the efficiency of this separation strategy, the Co and Ni contents of the two phases were evaluated via inductively coupled plasma optical emission spectroscopy (ICP-OES). In these triplicated experiments, the ammoniacal solution containing the 1:10 ratio of $[M(NH_3)_6][Cl]_x$ M = Co, Ni; x = 2, 3 was treated with 3 equiv of Na_2CO_3, and the resulting slurry was filtered through a medium porosity frit. The precipitate was washed with NH_4OH, and the washing was combined with the filtrate before analyzing the two phases for their metal content. As shown in **Table 1**, large separations factors ($\beta_{Co/Ni}$) were consistently observed for this procedure ($\beta_{Co/Ni}$ = 19,700 ± 1,200), with the precipitates recovering 76(10)% of Co with high purity (99.0(3))%) and the filtrates containing pure samples of Ni (99.4(2)% purity and 95(14)% recovery). In comparison, Cyanex 272, a well-studied commercial extractant for Co/Ni separations, has been reported to show $\beta_{Co/Ni}$ as high as 7000.[28] As a result, these separation factors are evidently competitive with state-of-the-art Co/Ni separations, and showcase the significant potential of this system towards application in industrial Co/Ni separations.

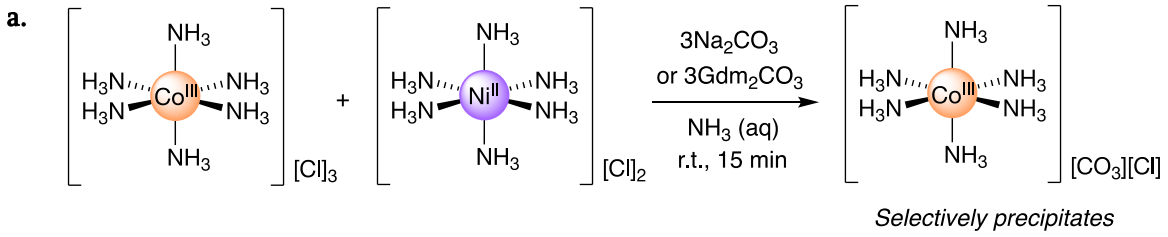

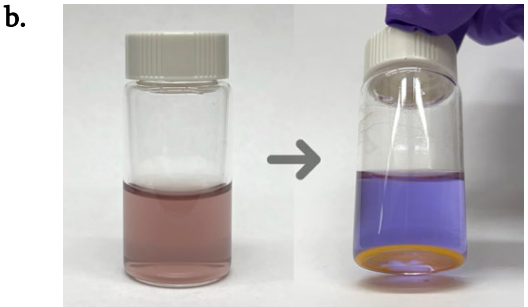

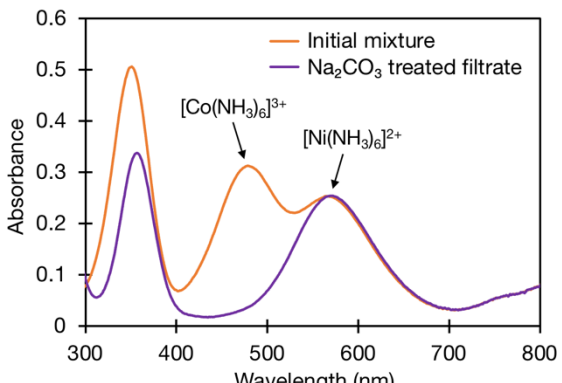

Fig. 3 Selective precipitation of cobalt from a mixture of Co/Ni$(NH_3)_6^{n+}$ n = 2, 3. a Scheme demonstrating the selective precipitation of cobalt from a Co/Ni mixture. **b** Photos of the Co/Ni complex mixture before (left) and after (right) treatment with Na_2CO_3. **c** UV-Vis spectra of the complex mixture before and after treatment of Na_2CO_3.

Table 1. Evaluation of Co/Ni separation by ICP-OES.

Starting Materials	Product	Purity	Recovery	$\beta_{Co/Ni}$
$[Co(NH_3)_6][Cl]_3$ and $[Ni(NH_3)_6][Cl]_2$	Co (in precipitate)	99.0(3)%	76(10)%	19700 ± 1200[a]
	Ni (in filtrate)	99.4(2)%	95(14)%	
$CoCl_2 \cdot 6H_2O$ and $NiCl_2 \cdot 6H_2O$	Co (in precipitate)	99.4(3)%	78(8)%	14000 ± 10000[b]
	Ni (in filtrate)	98.2(4)%	101(3)%	

[a] Separation factor was calculated from metals ratios in the solid versus solution phase starting from a 1:10 Co:Ni ratio. [b] The large uncertainty was due to the sensitivity of SF to minor changes at low metal concentrations. See SI for calculations.

Co/Ni separation from simple salt mixtures

The separation of pre-synthesized Co/Ni$(NH_3)_6^{n+}$ n = 2, 3 (*vide supra*) provided an important proof-of-concept separation. In a relevant separations scenario, the starting Co/Ni mixture would consist of simple salts of leachate the ions. Additionally, in the absence of strong L-type ligands, both metals would be expected to be divalent in the starting aqueous media. Next, we considered a more industrially-relevant separation starting from simple Co/$NiCl_2$ salts (**Fig. 4a**). As such, a 1:10 molar mixture of $CoCl_2 \cdot 6H_2O$ and $NiCl_2 \cdot 6H_2O$ was converted to $[Co^{III}(NH_3)_6][Cl]_3$ and $[Ni^{II}(NH_3)_6][Cl]_2$ *in situ* in the presence of NH_4OH, NH_4Cl, activated charcoal, and an oxidant (H_2O_2 or air). Spectral features in UV-Vis spectra of the reaction mixture matched those of the *bona fide* $[Co(NH_3)_6][Cl]_3$ and $[Ni(NH_3)_6][Cl]_2$ complexes (**Fig. 4b**). Violet crystals were obtained from the mixture when left at room temperature overnight, which were identified as $[Ni(NH_3)_6][Cl]_2$ using single crystal X-ray crystallography (**Supplementary Fig. 2**).

Following the formation of the mixture, additional concentrated NH_4OH and Na_2CO_3 (3 equiv) were added to selectively afford a yellow-orange precipitate, presumably $[Co(NH_3)_6][Cl][CO_3]$, upon stirring at r.t. for 20 min (**Fig. 4c**). Importantly, the addition of excess NH_4OH was necessary to stimulate precipitation, and to prevent partial redissolving of the precipitate over time. Powder X-ray diffraction (PXRD) was performed on the precipitate, and the resulting diffraction pattern displayed sharp diffraction peaks that closely matched those predicted from the solid-state structure of $[Co(NH_3)_6][Cl][CO_3]$ (**Fig. 4d**), thereby implying that the bulk

precipitate consists of this molecular solid. Thermogravimetric analysis (TGA) of the bulk precipitate material was performed yielded results that were consistent with the formula of molecular solid (See **Supplementary Information §4**). Finally, the applicability of the method at low concentrations of Co and Ni in starting materials was investigated: precipitation of cobalt (0.038 g, 49.5%) was observed at concentrations as low as 3 mM of $CoCl_2 \cdot 6H_2O$ (180 ppm Co) in the starting mixture.

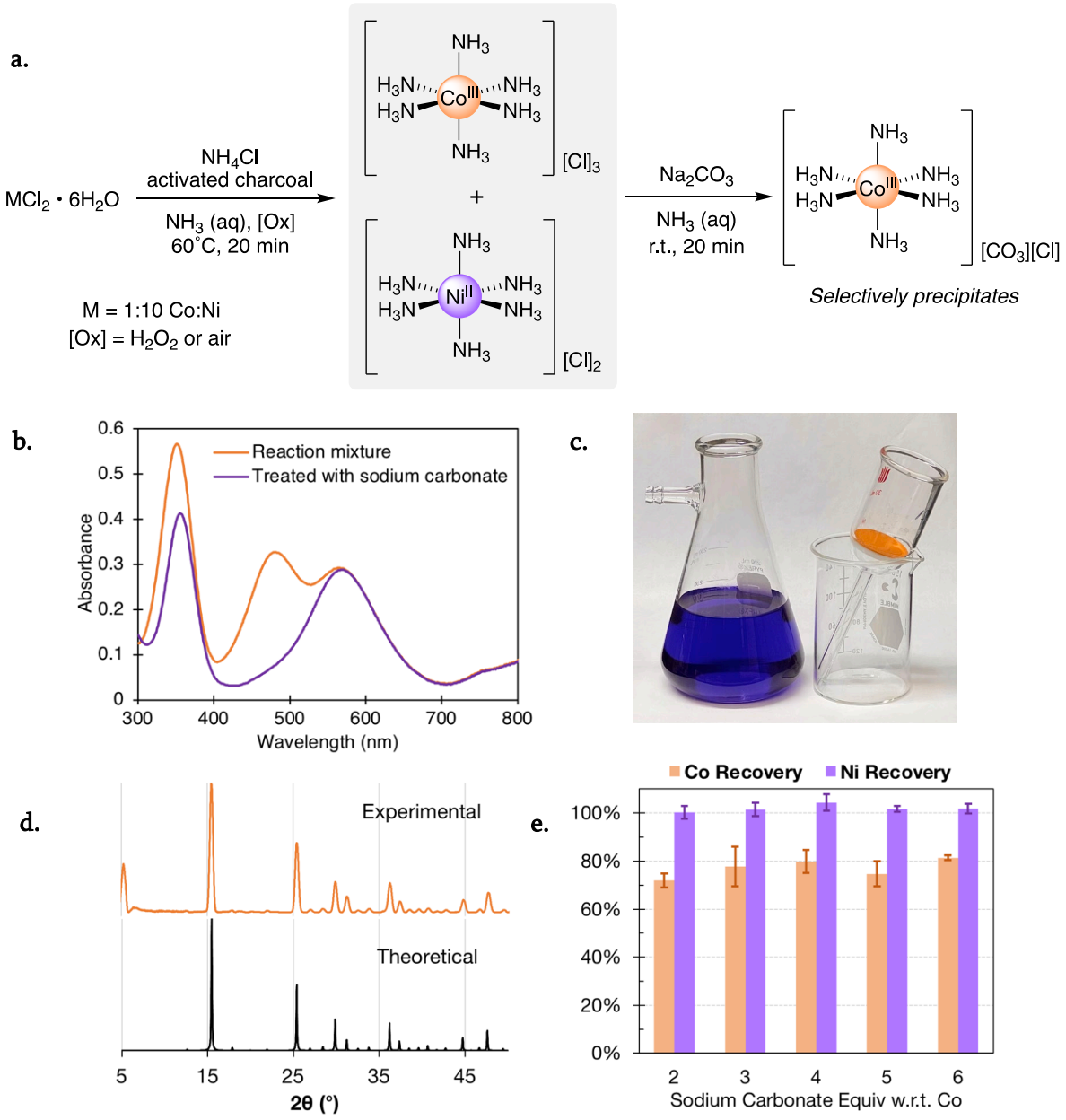

Fig. 4 Evaluation of selective cobalt precipitation using metal chlorides as starting materials. a Scheme outlining the separation method. **b** UV-Vis spectra of the reaction mixture before and after treatment with Na_2CO_3. **c** Photo of the yellow-orange precipitate collected on the fritted glass funnel and the remaining violet filtrate after filtration. **d** Experimental powder

X-ray diffraction pattern of the precipitate compared to the theoretical pattern of $[Co(NH_3)_6][Cl][CO_3]$. **e** Effect of Na_2CO_3 equivalents on the recovery of Co and Ni.

As before, the reaction was also characterized using UV-vis spectroscopy. Following precipitation of the orange-yellow solid, the remaining blue-violet filtrate displayed a spectral feature at 571 nm, corresponding to $[Ni(NH_3)_6][Cl]_2$. Additionally, the feature at 476 nm, corresponding to $[Co(NH_3)_6][Cl]_3$, was observed to bleach following the carbonated-induced precipitation event (**Fig. 4a**). Triplicated experiments were analyzed by ICP-OES, and they yielded comparable results to the previous separations starting from pre-synthesized $[Co/Ni(NH_3)_6][Cl]_x$ x = 2, 3 (**Table 1**), suggesting the viability of a one-pot strategy where the $[Co/Ni(NH_3)_6]^{n+}$ n = 2, 3 can be generated *in situ* followed by the carbonate precipitation. Increasing and decreasing the quantity of carbonate did not have a significant effect on these results (**Fig. 4e**), indicating that only minimal carbonate is necessary to impart the desired separation. The purities and recoveries of Co and Ni from these separations experiments are consistently high and further showcase the real-world application of this system to industrial Co/Ni separations.

Technoeconomic Analysis and Life-Cycle Assessment

An initial technoeconomic analysis (TEA)[29] of the Co/Ni separation was performed as a cost comparison with a previously deployed method, namely by solvent extraction (SX). It should be noted that few TEAs have been performed on mining/separations processes.[30,31] Our TEA approach was focused only on chemicals that distinguish the present Co/Ni separation from industrial SX processes. Since equipment for most of the recovery processes would be similar, it was estimated that equipment and energy costs would be comparable between processes. The least expensive chemicals that could be sourced from domestic or stable US trading partners were used within the TEA of the processes, and associated costs are tabulated in **Supplementary Table 11**. Due to the challenges associated with acquiring accurate industrial data, relevant ratios were obtained from the patent literature cited on the Queensland Nickel Incorporated (QNI) website for the Co/Ni SX separation process.[32,33] The QNI process **(Figure 6)** represents the closest approach, chemically, to the one presented in this work and was determined to be the best benchmark, with respect to equipment and energy usage.

The TEA-estimated cost of Co purification and recovery using the Co/Ni purification method described herein is 1.05 USD g^{-1}. In the previous QNI separation processes, several reagents are recycled, which decreases the associated costs. For the current process, a scaled recycling of Na_2CO_3, NH_4OH, and NH_4Cl have not yet been rigorously determined. This 1.05 USD g^{-1} cost estimate therefore represents an upper bound and would be expected to decrease with additional optimization. As a point of comparison, the TEA of the QNI SX process projects a price of 2.73 USD g^{-1} if reagent recycling is neglected. While this does not strictly represent a real-world comparison, it provides a rough estimate for how the two processes compare at similar levels of development. The chief cost difference between the two process is the use of hydrogen sulfide,

H_2S, used to form NH_4HS, in the QNI process, which is necessary for precipitating Co following the SX-based Co/Ni separation. The use of H_2S is both expensive and hazardous and it is known to poison the extractants used in the QNI-SX process, which impedes reagent/solvent recycling. In contrast, the carbonate-induced Co/Ni precipitation process removes the requirement for H_2S.

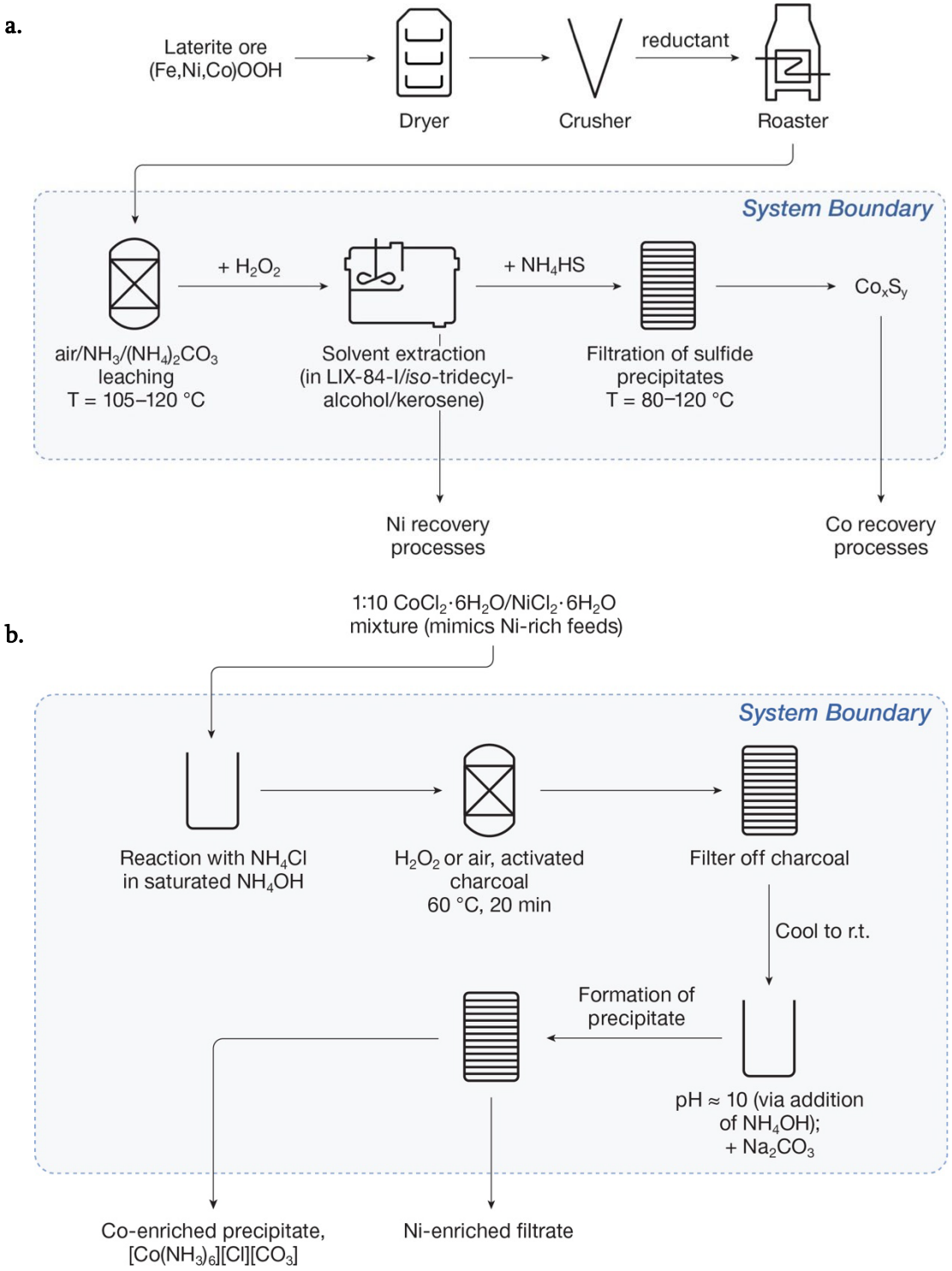

Fig. 6. Process flow diagrams for the **(a)** QNI process, and **(b)** the process reported in this work.

The TEA was also used to compare the environmental impacts of the two Co/Ni separation processes. Using current models in the Sustainable Materials Management (SMM) tool developed using Life-cycle Assessment (LCA) standards by the U.S. Environmental Protection Agency (EPA), the primary concerns in the Co/Ni supply chains were determined to be 1) respiratory effects and greenhouse gas (GHG) emissions associated with the smelting and purification processes, 2) substantial water use, and 3) contributions to acid rain from the use of volatile organic chemicals.[34] By targeting these supply chain hotspots, an appropriate comparison between the carbonate-induced separation process and the QNI-SX process was made. Using the academically-relevant assumption that approximately 0.1% of chemicals used in industrial processes escape into the environment,[35] replenishment and recharging of the solvents and extractants contribute significantly to the environmental cost of using SX at scale. Since EPA analyses pointed to respiratory concerns as well as airborne hazards, our initial LCA focused on Smog Formation Potential (SFP) and Human Toxicity by Inhalation Potential (INHTP). The simplified TEA and LCA are based on the same system boundaries and functional unit for direct comparison,[12,36,37] and these analyses are based on the average annual production of 31.3 kt of Co at Glencore.[38]

The SFP calculated (see **Supplementary Table 12**) in the initial stages of the LCA highlights a key benefit of the new method over SX processes: no volatile organic chemicals (VOC) are used. In SX processes, multiple extraction passes are performed to achieve sufficient Co/Ni purity, requiring the use of large quantities of solvents.[13,14,39] Both *iso*-tridecylalcohol and the kerosene diluent contribute to the SFP in the QNI process, totaling over 2.2×10^5 g ozone (O_3) equivalent chemicals being released. In contrast, 0 g of O_3 equivalent chemicals are released in the current process.

Human Toxicity by Inhalation Potential (INHTP), a key metric for inhalation hazards, also indicates benefit of the described carbonate process over the QNI process. Using the Multi-Compartmental Model (MCM),[40] the fraction of chemicals released into the atmosphere was calculated as compared to *all* released chemicals (both volatile and non-volatile). In the case of QNI-SX, *iso*-tridecylalcohol, LIX-84-I, kerosene, and H_2S all contribute to the INHTP calculation, whereas the current process only involves ammonia contributing to the calculation. Using parallel analyses, the QNI process resulted in an INHTP impact factor of 4.0×10^6, while the carbonate process scored more than an order of magnitude better, with an INHTP impact factor of 3.0×10^5.

Discussion

In this work, we present a simple method for separating mixtures Co/Ni by selective precipitation of: $[Co(NH_3)_6][Cl][CO_3]$ generated *in situ*. We demonstrate the potential of this method to serve as a sustainable, cost-effective alternative to traditional SX methods for the recovery of pure Co/Ni from either ore processing or battery recycling. The generation of the $[Co(NH_3)_6]^{3+}$ and $[Ni(NH_3)_6]^{2+}$ complexes is already applied industrially by an air/ammonia leaching technique, as previously employed at QNI, indicating potential for practical

development.[32] The current method offers advantages over existing acid leaching; acid leaching of Co and Ni is typically performed at elevated temperatures and pressures, which can be energy-intensive. The acid is also non-recyclable since it is neutralized in the subsequent chemical steps, leading to higher operational costs and large amounts of hazardous aqueous waste. For these reasons, ammoniacal leaching methods have also been proposed for LIB recycling.[41-45]

The simple and selective precipitation of Co presented in this work demonstrates potential for competing with currently adopted SX technologies, as indicated by the initial TEA. SX processes typically require multi-stage mixing/settling, and therefore require large solvent inventories. This requirement is reflected in the higher operational costs associated with SX methods compared to our new precipitation-based purification method. Additional optimization of the current proves is expected to deliver full recycling of the reagents used. For an example, one can envision ammoniacal leaching to be done under ambient conditions via injection of air and ammonia into a leaching liquor and/or LIB waste solution; dissolved ammonia in solution can then be readily recovered and reused. Since the Co-based network solid is soluble in neutral water, salt metatheses to recover carbonate from the purified Co should also be achievable.

Another useful benchmark for the current method is a selective leaching process to separate Co and Ni used currently at the Corefco refinery in Fort Saskatchewan, Canada, operated by Sherritt International.[46,47] Similar to the QNI SX, the Corefco process uses an air/ammonia leaching process to generate $[M(NH_3)_6]^{n+}$ M = Ni, Co; n = 2, 3. However, instead of solvent extraction, separation was achieved by leveraging the difference in solubility of $[Co(NH_3)_6]_2[SO_4]_3$ and $[Ni(NH_3)_6][SO_4]$ from NH_4OH solutions to deliver purities of 99.9% Co and 99.8% for Ni.[47] The Corefco process derives from roasting of mixed metal-sulfides such that it was tailored to a specific feed material. On the other hand, the use of the carbonate/chloride system disclosed here is more generalizable for different feeds and eliminates the potential for associated SO_x emissions.

In summary, the separation of Co/Ni from a mixture of simple Co/Ni salts can be achieved by *in situ* generation of $[Co(NH_3)_6]^{3+}$ and $[Ni(NH_3)_6]^{2+}$ species followed by selective precipitation of $[Co(NH_3)_6][Cl][CO_3]$ upon addition of a carbonate source. This strategy revisits the chemical differences in the classic hexammine "Werner" complexes of Co/Ni, and requires simple, inexpensive reagents and benign conditions while presenting competitive product purities and recovery. Lastly, we draw comparisons with existing industrial separation methods with the technoeconomic analysis and life-cycle assessment, demonstrating the benefits and potentials to adopt this strategy to separate Co and Ni from spent LIBs cathodes and ores.

Methods

Materials

The compounds $CoCl_2 \cdot 6H_2O$ (Thermo Scientific), $NiCl_2 \cdot 6H_2O$ (Thermo Scientific), NH_4Cl (99.5%, Thermo Scientific), Na_2CO_3 (Fisher Chemical), Gdm_2CO_3 (Acros), activated charcoal (Acros), ammonium hydroxide (28.0–30.0 w/w%, Fisher Chemical), and H_2O_2 (30%,

Fisher Chemical) were used as received. Ultra-pure water was generated by a Millipore Milli-Q system.

Synthesis of $[Co(NH_3)_6][Cl]_3$

$[Co(NH_3)_6][Cl]_3$ was prepared using a procedure adapted from the literature.[48] Briefly, $CoCl_2 \cdot 6H_2O$ (4.5 g, 19 mmol) and NH_4Cl (3.0 g, 56 mmol) were dissolved in water (5 mL) at 60˚C with stirring. The solution was cooled to 0˚C, to which activated charcoal (0.25 g, 21 mmol), NH_4OH (20 mL), and cold 30% H_2O_2 (20 mL, dropwise) were added. The mixture was heated to 60˚C with stirring for 20 min and then cooled to 0˚C. A black-brown precipitate was obtained upon filtration and was then dissolved in 40 mL of boiling water mixed with 1.5 mL of 12 M HCl. The hot solution was immediately filtered. Upon cooling the red-orange filtrate to 0˚C, an orange solid formed and was collected via filtration. The solid was washed with cold water (2 mL) and acetone (3 mL) before drying under vacuum. Yield: 2.7 g, 54%.

Synthesis of $[Ni(NH_3)_6][Cl]_2$

$NiCl_2 \cdot 6H_2O$ (30.0 g, 126 mmol) and NH_4Cl (6.78 g, 126 mmol) were dissolved in water (10 mL). To the green solution was added NH_4OH (150 mL). The mixture immediately turned violet and was stirred at r.t. for 20 min. A violet solid was obtained upon filtration and was then washed with 5 × 5 mL cold NH_4OH, followed by 3 × 10 mL diethyl ether. The solid was dried under vacuum for 4 h. Yield: 24.6 g, 84%.

***In Situ* Generation of the $[Co(NH_3)_6][Cl]_3$ and $[Ni(NH_3)_6][Cl]_2$ Mixture**

$CoCl_2 \cdot 6H_2O$ (0.301 g, 1.27 mmol, 1 equiv), $NiCl_2 \cdot 6H_2O$ (2.996 g, 12.6 mmol, 10 equiv) were dissolved in 6 mL of deionized water. The mixture was sonicated until the metal salts dissolved completely to form a dark green solution. NH_4Cl (2.024 g, 37.8 mmol, 30 equiv) and activated charcoal (0.167 g, 13.9 mmol, 11 equiv) was subsequently added, followed by dropwise addition of 20 mL of NH_4OH which led to an immediate color change to violet. The mixture was then subjected to oxidation via one of the two methods below.

Method 1: Using H_2O_2. In an ice bath, to the flask was slowly added 20 mL of cold 30% H_2O_2 dropwise over *ca.* 2 min with stirring (200 rpm). An exothermic reaction with effervescence immediately occurred. The mixture was stirred (200 rpm) at 0˚C for 20 min and then at room temperature for 20 min.

Method 2: Using Aeration. An additional 40 mL of NH_4OH was added to the mixture to compensate for the loss of ammonia due to aeration. A glass pipette was then submerged in the solution to pass air through the mixture for 3 h.

The mixture was then heated to 60˚C in a water bath with stirring for 20 min, and the charcoal was removed by filtering the hot solution over a Büchner funnel. An additional 180 mL of NH_4OH was immediately added to the dark magenta filtrate.

UV-Vis: λ = 476 nm ($[Co(NH_3)_6][Cl]_3$), λ = 571 nm ($[Ni(NH_3)_6][Cl]_2$).

Separation of $[Co(NH_3)_6][Cl][CO_3]$

Na_2CO_3 (following Method 1: 0.401 g, 3.78 mmol, 3 equiv) was added to the dark magenta filtrate containing $[Co(NH_3)_6][Cl]_3$ and $[Ni(NH_3)_6][Cl]_2$ from above. Upon stirring at 650 rpm for 20 minutes at room temperature, a yellow-orange precipitate gradually formed. The solid was collected by filtering the slurry over a medium porosity fritted funnel and was subsequently washed with 3 × 3 mL of NH_4OH. The precipitate was dried overnight at 40˚C in an electric oven before being removed from the funnel. Yield: 0.297g, 83.2%. (%yield = mass of the isolated precipitate / expected mass of $[Co(NH_3)_6][Cl][CO_3]$).

UV-Vis spectroscopy

UV-Vis absorption spectra were collected in NH_4OH at room temperature, on a Perkin Elmer 950 UV-Vis/NIR spectrophotometer with quartz cells (10 mm path length). Background subtraction was done using blank scans of NH_4OH.

Crystallization and single-crystal X-ray diffraction analysis

Crystalline samples of $[Co(NH_3)_6][Cl][CO_3]$ of single crystal quality were prepared by combining a solution of Na_2CO_3 (0.064 g, 0.30 mmol) and a solution of $[Co(NH_3)_6][Cl]_3$ (0.081 g, 0.60 mmol) in NH_4OH (10 mL) in a scintillation vial. Yellow-orange precipitate formed immediately. The vial was left uncapped at ambient conditions for several days until orange crystals formed.

X-ray intensity data were collected on a Rigaku XtaLAB Synergy-S diffractometer equipped with an HPC area detector (HyPix-6000HE) and employing confocal multilayer optic-monochromated Mo-Kα radiation (λ=0.71073 Å) at a temperature of 100 K. See **Supplementary Information §3** for full details.

Powder X-ray diffraction analysis

Powder XRD were collected using a Rigaku XtaLAB Synergy-S diffractometer equipped with an HPC area detector (HyPix-6000HE) and employing confocal multilayer optic-monochromated Mo-Kα radiation (λ=0.71073 Å) or Cu-Kα radiation (λ=1.54184 Å) at a temperature of 100K. The simulated PXRD pattern was calculated using Mercury software 2023.1.0.

Inductively coupled plasma optical emission spectroscopy

Co and Ni content in the samples were quantified by using a Spectro Genesis ICP-OES spectrometer controlled by SmartAnalyzer Vision program. The spectrometer was equipped with an integrated three channel peristaltic pump, a CETAC ASX-260 auto-sampler, a Modified Lichte nebulizer chamber, and a 2.5 mm torch injector. Standard solutions for calibrations were prepared by performing dilutions of 1000 µg/mL Specpure® cobalt and nickel plasma standard solutions purchased from Thermo Scientific. Ultra-pure water was used as blank. Emission wavelengths chosen for analyses were Co 230.786 nm and Ni 221.648 nm. Additional details including instrument operating parameters can be found in **Supplementary Information §6**.

Aliquots and portions were taken from the isolated filtrate and precipitate respectively, and aqueous aliquots were dried under vacuum prior to next steps. All samples were heated at 300˚C using a sand bath for 30 min and allowed to cool to room temperature. Finally, samples were digested in 5 mL of concentrated HCl at room temperature overnight, followed by dilution with ultra-pure water.

Computational analysis

See **Supplemental Information §8.4**.

Acknowledgements

M.G. thanks Dr. Warren D. Seider at the University of Pennsylvania and Dr. Geetanjali Yadav at the National Renewable Energy Laboratory for their help with the technoeconomic analysis. B.Z. thanks Dr. David Burney at the University of Pennsylvania for his kind assistance with ICP-OES. E.J.S. acknowledges the Center for Sustainable Separations of Metals (CSSM), a National Science Foundation Center for Chemical Innovation under award number CHE-1925708, for initial support of this work. E.J.S. also acknowledges the University of Pennsylvania for support.

Author Contributions

A.B.W. and B.Z. conceived this project. A.B.W. carried out key preliminary separation studies. B.Z. developed and optimized the separation method from metal chlorides. M.G. conducted the technoeconomic analysis and life-cycle assessment. L.O.J. and G.C.S. conducted the theoretical computations. M.R.G. and P.J.C. collected and solved the X-ray structures and PXRD patterns. A.J.A. assisted in the experiments and contributed to the writing of the manuscript. E.J.S. provided guidance and supervised the research. A.B.W., B.Z., A.J.A., M.G., L.O.J., and E.J.S. participated in drafting the manuscript. All authors discussed the results and contributed to the preparation of the manuscript.

Competing Interests

The authors declare the following competing financial interest: Intellectual property pertaining to the technology described in this article is covered by International Patent Application no. PCT/US2024/020243.

Data Availability

Crystallographic data for the structures reported in this article have been deposited at the Cambridge Crystallographic Data Center (CCDC) under deposition nos. CCDC XXXXXXX (XXXX) and XXXXXXX (XXX). These data can be obtained free of charge from the Cambridge Crystallographic Data Centre via www.ccdc.cam.ac.uk/data_request/cif. All

other data supporting the findings of this study are available within the Article and its Supplementary Information and from the corresponding authors upon reasonable request.

References

1 International Energy Agency. The Role of Critical Minerals in Clean Energy Transitions. (International Energy Agency, Paris, 2021).

2 Ambrose, H. & Kendall, A. Effects of battery chemistry and performance on the life cycle greenhouse gas intensity of electric mobility. *Transportation Research Part D: Transport and Environment* **47**, 182-194 (2016). https://doi.org:10.1016/j.trd.2016.05.009

3 Harper, G. *et al.* Recycling lithium-ion batteries from electric vehicles. *Nature* **575**, 75-86 (2019). https://doi.org:10.1038/s41586-019-1682-5

4 Kim, K., Raymond, D., Candeago, R. & Su, X. Selective cobalt and nickel electrodeposition for lithium-ion battery recycling through integrated electrolyte and interface control. *Nat. Commun.* **12**, 6554 (2021). https://doi.org:10.1038/s41467-021-26814-7

5 Cheng, A. L., Fuchs, E. R. H., Karplus, V. J. & Michalek, J. J. Electric vehicle battery chemistry affects supply chain disruption vulnerabilities. *Nat. Commun.* **15**, 2143 (2024). https://doi.org:10.1038/s41467-024-46418-1

6 Cobalt Institute. Cobalt Market Report 2021. (Zurich, 2022).

7 U.S. Geological Survey. Mineral Commodity Summaries 2023. (U.S. Geological Survey, Reston, Virginia, 2023).

8 Farjana, S. H., Huda, N. & Mahmud, M. A. P. Life cycle assessment of cobalt extraction process. *Journal of Sustainable Mining* **18**, 150-161 (2019). https://doi.org:10.1016/j.jsm.2019.03.002

9 Gross, T. How 'modern-day slavery' in the Congo powers the rechargeable battery economy. *NPR* (2023). <https://www.npr.org/sections/goatsandsoda/2023/02/01/1152893248/red-cobalt-congo-drc-mining-siddharth-kara>.

10 Mayyas, A., Steward, D. & Mann, M. The case for recycling: Overview and challenges in the material supply chain for automotive li-ion batteries. *Sustainable Materials and Technologies* **19**, e00087 (2019). https://doi.org:https://doi.org/10.1016/j.susmat.2018.e00087

11 Peters, J. F., Baumann, M., Zimmermann, B., Braun, J. & Weil, M. The environmental impact of Li-Ion batteries and the role of key parameters – A review. *Renewable and Sustainable Energy Reviews* **67**, 491-506 (2017). https://doi.org:10.1016/j.rser.2016.08.039

12 Slack, J. F., Kimball, B. E. & Shedd, K. B. in *Critical Mineral Resources of the United States—Economic and Environmental Geology and Prospects for Future Supply* (eds Klaus J. Schulz, John H. DeYoung, Jr., Robert R. Seal, II., & Dwight C. Bradley) (U.S. Geological Survey, Reston, VA, 2017).

13 Flett, D. S. Cobalt-nickel separation in hydrometallurgy: a review. *Chemistry for sustainable development* **12**, 81-91 (2004).

14 Alvial-Hein, G., Mahandra, H. & Ghahreman, A. Separation and recovery of cobalt and nickel from end of life products via solvent extraction technique: A review. *Journal of Cleaner Production* **297**, 126592 (2021). https://doi.org:10.1016/j.jclepro.2021.126592

15 Liu, Z. *et al.* Selective isolation of gold facilitated by second-sphere coordination with α-cyclodextrin. *Nat. Commun.* **4**, 1855 (2013). https://doi.org:10.1038/ncomms2891

16 Doidge, E. D. *et al.* A Simple Primary Amide for the Selective Recovery of Gold from Secondary Resources. *Angew. Chem. Int. Ed.* **55**, 12436-12439 (2016). https://doi.org:https://doi.org/10.1002/anie.201606113

17 Chen, L.-X. *et al.* Outer surface interactions to drive cucurbit[8]uril-based supramolecular frameworks: possible application in gold recovery. *Chem. Commun.* **55**, 14271-14274 (2019). https://doi.org:10.1039/C9CC07147D

18 Wu, H. *et al.* High-Efficiency Gold Recovery using Cucurbit[6]uril. *ACS Applied Materials & Interfaces* **12**, 38768-38777 (2020).
19 Kinsman, L. M. M., Ngwenya, B. T., Morrison, C. A. & Love, J. B. Tuneable separation of gold by selective precipitation using a simple and recyclable diamide. *Nat. Commun.* **12**, 6258 (2021). https://doi.org:10.1038/s41467-021-26563-7
20 O'Connell-Danes, J. *et al.* Shape-Selective Supramolecular Capsules for Actinide Precipitation and Separation. *JACS Au* **4**, 798-806 (2024). https://doi.org:10.1021/jacsau.3c00793
21 O'Connell-Danes, J. G., Ngwenya, B. T., Morrison, C. A. & Love, J. B. Selective separation of light rare-earth elements by supramolecular encapsulation and precipitation. *Nat. Commun.* **13**, 4497 (2022). https://doi.org:10.1038/s41467-022-32178-3
22 Wu, H. *et al.* High-efficiency gold recovery by additive-induced supramolecular polymerization of β-cyclodextrin. *Nat. Commun.* **14**, 1284 (2023). https://doi.org:10.1038/s41467-023-36591-0
23 Wiesendanger, H. U. D., Jones, W. H. & Garner, C. S. Exchange of Ammonia between Metal-Ammine Cations and Solvent in Liquid Ammonia. *The Journal of Chemical Physics* **27**, 668-672 (1957). https://doi.org:10.1063/1.1743811
24 Llewellyn, D. R., O'Connor, C. J. & Odell, A. L. 32. Exchange reactions of Co-ordinated ammonia: isotopic study of the lability of ammines of copper(II), nickel(II), platinum(II), chromium(III), and cobalt(III) in aqueous solution. *Journal of the Chemical Society (Resumed)*, 196-200 (1964). https://doi.org:10.1039/JR9640000196
25 Rutenberg, A. C. & Drury, J. S. The Exchange of Ammonia between Aqueous Ammonia and Co(NH3)6Cl3. *Inorg. Chem.* **2**, 219-219 (1963). https://doi.org:10.1021/ic50005a057
26 Pyrch, M. M. F. *et al.* Investigations of the Cobalt Hexamine Uranyl Carbonate System: Understanding the Influence of Charge and Hydrogen Bonding on the Modification of Vibrational Modes in Uranyl Compounds. *Inorg. Chem.* **61**, 15023-15036 (2022). https://doi.org:10.1021/acs.inorgchem.2c01982
27 Liu, W. Q. *et al.* Supramolecular Gold Stripping from Activated Carbon Using α-Cyclodextrin. *Journal of the American Chemical Society* **143**, 1984-1992 (2021). https://doi.org:10.1021/jacs.0c11769
28 Flett, D. S. Solvent extraction in hydrometallurgy: the role of organophosphorus extractants. *J. Organomet. Chem.* **690**, 2426-2438 (2005). https://doi.org:https://doi.org/10.1016/j.jorganchem.2004.11.037
29 Langhorst, T. *et al.* Techno-Economic Assessment & Life Cycle Assessment Guidelines for CO2 Utilization (Version 2.0). (2022).
30 Chen, Y. *et al.* Selective recovery of precious metals through photocatalysis. *Nature Sustainability* **4**, 618-626 (2021). https://doi.org:10.1038/s41893-021-00697-4
31 Stinn, C. & Allanore, A. Selective sulfidation of metal compounds. *Nature* **602**, 78-83 (2022).
32 Price, M. J. & Reid, J. G. Separation and recovery of nickel and cobalt in ammoniacal systems. AU605867B2 (1987).
33 Ferguson, E. S. P., M. J.; Reid, J. G. Two Phase Oxime Synthesis. Australia patent AU 612528 (1989).
34 U.S. Environmental Protection Agency. *Sustainable Material Management Prioritization Tool*, <https://www.epa.gov/smm/organizational-smm-prioritization-tool> (2022).
35 Mercer, S. M. A., J.; Jessop, P. G. . Choosing the Greener Synthesis: A Multivariate Metric Green Chemistry Exercise. *J. Chem. Educ.* **89**, 215-220 (2012). https://doi.org:10.1021/ed200249v
36 Horn, S. *et al.* Cobalt Resources in Europe and the Potential for New Discoveries. *Ore Geology Reviews* **130**, 103915 (2021).
37 Commission, E. Study on the EU's list of Critical Raw Materials (2020) : final report. . *Directorate General for Internal Market* (2020).
38 Glencore. <https://www.glencore.com/what-we-do/metals-and-minerals/cobalt > (2022).
39 Queensland Nickel. *Operational Overview*, <https://www.qni.com.au/about-qn/operational-overview/> (

40 Mackay, D. S., W-Y.; Ma, K-C; Lee, S.C. *Handbook of Physical-Chemical Properties and Environmental Fate for Organic Chemicals*. 2nd edn, (CRC Press, 2006).
41 Wang, S., Wang, C., Lai, F., Yan, F. & Zhang, Z. Reduction-ammoniacal leaching to recycle lithium, cobalt, and nickel from spent lithium-ion batteries with a hydrothermal method: Effect of reductants and ammonium salts. *Waste Manage. (Oxford)* **102**, 122-130 (2020). https://doi.org:10.1016/j.wasman.2019.10.017
42 Ku, H. *et al.* Recycling of spent lithium-ion battery cathode materials by ammoniacal leaching. *J. Hazard. Mater.* **313**, 138-146 (2016). https://doi.org:10.1016/j.jhazmat.2016.03.062
43 Liu, X., Huang, K., Xiong, H. & Dong, H. Ammoniacal leaching process for the selective recovery of value metals from waste lithium-ion batteries. *Environ. Technol.* **44**, 211-225 (2023). https://doi.org:10.1080/09593330.2021.1968505
44 Wang, H. *et al.* Recovery of Lithium, Nickel, and Cobalt from Spent Lithium-Ion Battery Powders by Selective Ammonia Leaching and an Adsorption Separation System. *ACS Sustainable Chem. Eng.* **5**, 11489-11495 (2017). https://doi.org:10.1021/acssuschemeng.7b02700
45 Wang, C. *et al.* Recycling of spent lithium-ion batteries: Selective ammonia leaching of valuable metals and simultaneous synthesis of high-purity manganese carbonate. *Waste Manage. (Oxford)* **114**, 253-262 (2020). https://doi.org:10.1016/j.wasman.2020.07.008
46 Kerfoot, D. G. E. Process for the separation of cobalt from nickel. US5468281A (1995).
47 Cordingley, P. D. & Krentz, R. in *Nickel and Cobalt 2005: Challenges in Extraction and Production* (eds J. Donald & R. Schonewille) 407–425 (CIM, 2005).
48 Bjerrum, J. & McReynolds, J. P. in *Inorg. Synth.* Vol. II (ed W. Conard Fernelius) 216–221 (McGraw-Hill Book Company, 1946).